

Excited state proton transfer in the S_1 state of 2-allylphenol, 2-propenylphenol, and 2-propylphenol and their van der Waals clusters with water and ammonia

S. K. Kim, S. C. Hsu, S. Li, and E. R. Bernstein

Citation: *The Journal of Chemical Physics* **95**, 3290 (1991); doi: 10.1063/1.460835

View online: <http://dx.doi.org/10.1063/1.460835>

View Table of Contents: <http://aip.scitation.org/toc/jcp/95/5>

Published by the *American Institute of Physics*

COMPLETELY

REDESIGNED!



**PHYSICS
TODAY**

Physics Today Buyer's Guide
Search with a purpose.

Excited state proton transfer in the S_1 state of 2-allylphenol, 2-propenylphenol, and 2-propylphenol and their van der Waals clusters with water and ammonia

S. K. Kim,^{a)} S. C. Hsu,^{b)} S. Li, and E. R. Bernstein

Colorado State University, Chemistry Department, Fort Collins, Colorado 80523

(Received 12 March 1991; accepted 20 May 1991)

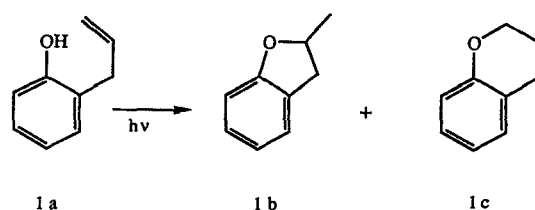
Excited state intramolecular and intermolecular proton transfer reactions in cold, isolated 2-allylphenol, 2-propenylphenol and 2-propylphenol, and their clusters with water and ammonia are investigated employing a combination of spectroscopic techniques (mass resolved excitation, threshold photoionization, dispersed emission), a semiempirical calculation (MOPAC 5) and a potential energy calculation of cluster structure. Threshold photoionization spectroscopy proves to be useful for the identification of molecular conformers in these systems but has mixed results for the identification of proton transfer in their clusters. The total collection of generated data suggests the following conclusions: (1) isolated, cold 2-allylphenol displays only one conformation which appears to have a significant stabilizing intramolecular interaction between the allyl group double bond and the hydroxyl group hydrogen atom; (2) 2-propenylphenol displays only one conformer; (3) 2-propylphenol has many conformations—probably more than five under the experimental conditions; (4) no evidence of intramolecular proton transfer can be found for these three isolated cold molecules; (5) no evidence for intermolecular proton transfer in water clusters has been found by any of the above techniques; and (6) evidence is found for intermolecular proton transfer in 2-allyl⁻ and 2-propenylphenol(NH_3)_n, $n \geq 3$, in dispersed emission spectra. Dispersed emission spectra of 2-propylphenol(NH_3)_n, $n \geq 3$ are too weak to yield conclusive evidence for intermolecular excited state proton transfer. Potential energy minimization calculations of cluster geometry suggest that the difference between water and ammonia cluster behavior with regard to proton transfer arises because water molecules hydrogen bond with the hydroxyl group (both $\text{OH} \cdots \text{OH}_2$ and $\text{HO} \cdots \text{HOH}$) and each other while ammonia molecules are more evenly distributed over the entire molecular structure of the phenol moiety. Apparently, for efficient proton transfer to occur in clusters, the proton affinity of the solvent must be large and both the anion and the proton must be well solvated (stabilized) by the solvent.

I. INTRODUCTION

The study of chemical reactions in cold, isolated van der Waals clusters has begun to make important contributions to the understanding of reaction mechanisms and dynamics.¹ Since cluster size, and to some extent cluster structures, can be controlled and/or selectively accessed in isolated clusters, the process of solvation and the effects of solvation on chemical reactions can be readily accessed in clusters.

A particularly interesting and apparently straightforward reaction for study in clusters is the elementary acid-base proton transfer reaction. Molecules which possess an aromatic hydroxyl group are attractive candidates for these reactions because they undergo large changes in pK_a upon photoexcitation from the ground (S_0) to the first excited single $t(S_1)$ state. For example, a Förster cycle² calculation for phenol gives $\text{pK}_a(S_0) \sim 10.0$ and $\text{pK}_a(S_1) \sim 3.6$.^{3,4} Substitution of halo, allyl, and alkoxy groups on the phenol yield little change for these pK_a values while nitrosubstituted phenols evidence increased acidity changes upon photoexcitation.³

In orthosubstituted phenols both intra- and intermolecular proton transfer can take place upon solution phase photoexcitation: 2-allylphenol [see **1(a)** in Scheme I] provides a good example of such behavior. 2-allylphenol is known to photoisomerize to generate cyclic ethers [**1(b)** and **1(c)**] in nonpolar solutions⁵⁻⁷ as shown in Scheme I. The reaction is suggested to proceed via an intramolecular proton transfer between the hydroxyl hydrogen and the allyl group double bond.



Scheme I

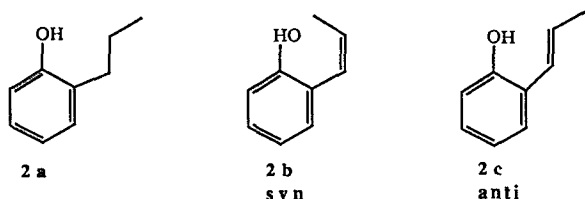
This photoinduced intramolecular proton transfer is suppressed in protic solvents.⁶ Intermolecular proton transfer prevails in protic solutions. If the solvent proton affinity could be carefully tuned or controlled, intra- and intermole-

^{a)} Current address: Code 6546, Naval Research Laboratory, Washington, D.C. 20375-5000.

^{b)} Current address: Shell Development Company, Westhollow Research Center, Houston, Texas 77082.

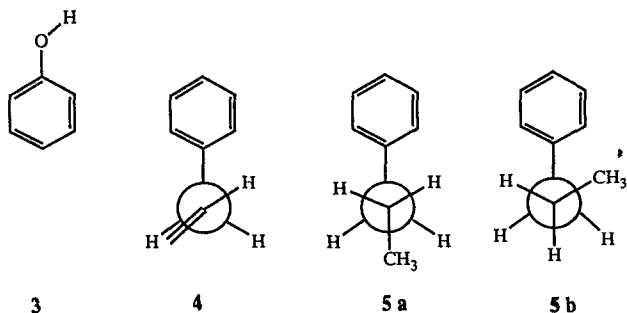
cular transfer might both be observed. While this possibility has not been realized in liquid solvation, the two different photoinduced proton transfer reactions might coexist under isolated conditions for appropriately structured clusters. Will 2-allylphenol undergo intra- or intermolecular proton transfer in water and ammonia clusters? Can one determine if the transfer is intra- or intermolecular?

The interaction between the phenol hydroxyl group and the 2-substituent on the ring, and thus the probability of intramolecular proton transfer, can be varied by changing the nature of the 2-substituent. Thus 2-propenyl and 2-propylphenol can be investigated along with 2-allylphenol. In solution, no cyclization reaction is found for 2-propylphenol (**2a**) and 2-propenylphenol (**2b**, **2c**) undergoes cyclization (see Scheme I) only in the presence of a palladium catalyst.⁸ The series of molecules **1a**, **2a**, **2b**, **2c** thus should allow one to distinguish between intra- and intermolecular proton transfer in van der Waals clusters under controlled solvation conditions.



The above 2-substituted phenols can be expected to exist in a number of different molecular conformations when cooled in a supersonic expansion: solute/solvent van der Waals clusters of a given mass containing these species will display multiple conformations, as well. Thus intra- and intermolecular proton transfer can be investigated as a function of molecular geometry, cluster geometry, and number of solvent molecules present in the cluster.

The conformations of the related aromatic molecules containing only single substituents are already determined: (1) the OH group in phenol (**3**) is contained in the plane of the aromatic ring;⁹ (2) the allyl group of allylbenzene (**4**) has the $C_\alpha-C_\beta$ bond perpendicular to the plane of the aromatic ring and the allyl group double bond is eclipsed with one of the $C_\alpha-H$ bonds;¹⁰ (3) the entire heavy atom structure is planar for propenylbenzene (β -methylstyrene);¹¹ and (4) the propyl group in propylbenzene (**5**) has the $C_\alpha-C_\beta$ bond perpendicular to the plane of the aromatic ring and the $C_\beta-C_\gamma$ bond can be both *anti* and *gauche* to the ring.¹² These structures are expected to be altered to some degree in 2-substituted phenols due to steric and hydrogen bonding interactions.



Supersonic jet spectroscopy of molecules with multiple conformations becomes somewhat more complicated than usual. A number of techniques can be employed to distinguish different conformers of molecules from low lying vibronic features: (1) isotopic substitution will often yield large effects on vibronic features (e.g., shifts of greater than 5% in S_1 vibrations) but only small changes in conformer origins;¹³ (2) hole-burning experiments can be used to identify features (0_0^0 , X_0^1 , etc.) common to a particular conformer;¹⁴ and (3) ionization threshold measurements can demonstrate that conformers of a given molecule can have somewhat different ionization energies.¹⁵

The latter technique of threshold photoionization can also be important for cluster studies and the identification of chemical reactions in clusters.¹⁶⁻¹⁸ Clusters of different structures can have different ionization energies [e.g., (pyrazine)₂, (pyrimidine)₂, etc.,¹⁹ and naphthol/H₂O and NH₃¹⁸]. Clusters which have undergone proton transfer (e.g., naphthol/NH₃) can also have a dramatically reduced ionization energy.¹⁶⁻¹⁸

This paper reports five separate studies on the 2-allyl-, 2-propenyl-, and 2-propyl-phenol molecules and their clusters with ammonia and water: mass resolved excitation spectroscopy; dispersed emission spectroscopy; threshold photoionization spectroscopy; semiempirical modified neglect of diatomic overlap (MNDO) calculations (MOPAC 5) of molecular structure; and cluster potential energy minimization calculations. Based on these results, we determine that only intermolecular excited state (S_1) proton transfer occurs for solute(NH₃)_n, $n \geq 3$ clusters.

II. EXPERIMENTAL PROCEDURES

A more detailed description of the supersonic jet apparatus and time of flight mass spectrometer employed in this effort can be found in earlier publications from our laboratory.²⁰ One-color mass resolved excitation spectroscopy (MRES) provides only crowded spectra for the samples used in this study probably due to extensive fragmentation from clusters of these molecules with impurity water. The ionization wavelength for two-color MRES is chosen to be low enough such that no cluster fragmentation is observed.

Threshold photoionization spectra are obtained with the $S_1 \leftarrow S_0$ excitation energy (ν_{ex}) fixed for a particular transition and the $I \leftarrow S_1$ ionization energy (ν_{ion}) scanned. The mass spectrometer extraction field for the created ions is ~ 100 V/cm. The threshold photoionization value reported for the isolated molecules is obtained as follows: the spectrum is smoothed with Fourier transform filtering and the wavelength for the maximum signal derivative is found. The FWHM of the derivative function is reported as the width of the onset. Cluster signal intensities are smaller and the threshold spectra are quite broad; for these signals the detected onset of the ionization signal is reported for the threshold value.

2-allylphenol, 2-propenylphenol, and 2-propylphenol are purchased from Aldrich Co. These samples are quite hygroscopic and contain $\sim 2\%$ water as an impurity. Two-color mass resolved excitation spectra of these species are not influenced by this difficulty: a problem, of course, arises

for dispersed emission studies which are not mass selective. Samples are dried in vacuum over P_2O_5 . Even for dried 2-propylphenol, the dispersed emission spectrum contains mostly 2-propylphenol/ H_2O features. We are not able to obtain dispersed emission spectra of 2-propylphenol or 2-propylphenol/ammonia clusters free of water cluster contamination. The dispersed emission spectra for 2-allyl- and 2-propenylphenols and their ammonia clusters can be obtained free of interference from water cluster features.

The sample of 2-propenylphenol contains 80% anti-[2(c)] and 20% [2(b)] syn-isomers as determined by ^{13}C - and 1H -NMR spectroscopy.

Samples are placed in the head of a pulsed nozzle and heated to $\sim 40^\circ C$. 50 psi. He is typically employed as the expansion gas.

Fluorescence from these samples is weak so dispersed emission spectra are taken with uv cutoff filters placed in front of a photomultiplier tube detector. The filters used are Hoya UV22, UV28, UV30, UV32, UV34, UV36, L38, and L40. This technique provides ~ 20 nm resolution dispersed emission spectra. The figure caption for the dispersed emission spectra of these systems contains transmission information for the filters.

Geometries for the 2-substituted phenols are calculated employing a semiempirical MNDO algorithm, MOPAC 5 using PM3 and AM1 Hamiltonians.²¹ Both calculations give the same results and thus only the PM3 results are reported herein. Starting geometries are varied to locate all minima on the potential surface for both the hydroxyl group and the hydrocarbon side chain. Stringent convergence criteria ($GNORM = 0.01$) still yield many minima for each molecule.

Cluster structures are also calculated employing the MOPAC 5 charges and minimum energy molecular geometries and a cluster energy minimization routine previously described.²²

III. RESULTS

A. 2-Allylphenol

1. MRES and threshold photoionization of the isolated molecule

Two-color MRES of the 2-allylphenol $S_1 \leftarrow S_0$ transition origin region is shown in Fig. 1(a). The lowest energy intense feature is at $36\,029\text{ cm}^{-1}$ (peak A) and is assigned as a 0_0^0 transition for a conformer of 2-allylphenol. This origin has a 50 cm^{-1} harmonic progression built on it. Figure 1(b) demonstrates that this 50 cm^{-1} progression built on the 2-allylphenol origin must be due to motion of the allyl group because deuteration of the hydroxyl group does not change the progression spacing. Features labeled B and C in Fig. 1 can be associated with low energy ring modes. No other electronic origins (conformers) have been identified for 2-allylphenol.

The $I \leftarrow S_1$ photoionization spectrum for the peak A has a sharp ($\Delta\nu_{\text{ion}} = 22\text{ cm}^{-1}$) onset at $\nu_{\text{ion}} = 29\,662 \pm 4\text{ cm}^{-1}$ (Fig. 2). These observations and assignments are summarized in Table I.

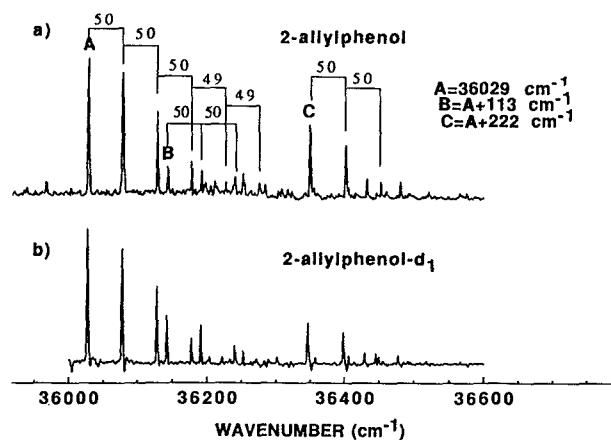


FIG. 1. 2-color MRES of 2-allylphenol: (a) Peak intensities are calibrated with dye curves of the excitation laser. Frequency of ionizing laser (ν_{ion}) is $29\,800\text{ cm}^{-1}$; (b) 2-color MRES of 2-allylphenol- d_1 for comparison with (a).

2. MRES and threshold photoionization of water and ammonia clusters

Two-color MRES are displayed in Fig. 3 for 2-allylphenol(H_2O)_{1,2}. The four different spectral regions displayed in Fig. 3(a) can probably be associated with 2-allylphenol(H_2O)₁ clusters of different structure. This point is best made by the threshold photoionization data presented in Table II. Most of the vibronic structure displayed in these spectra is due to allyl group motion: expansion of 2-allylphenol with D_2O does not change any of the observed spectra. The 2-allylphenol(H_2O)₂ spectra displayed in Fig. 3(b) are much simpler and show less structural diversity than do those of the 1:1 cluster. This observation will be rationalized later in light of cluster structure calculations and through comparison with results for 1-naphthol/water and ammonia clusters.¹⁸

The 2-allylphenol(H_2O)₁ cluster absorbing $\sim 35\,000\text{ cm}^{-1}$ [Fig. 3(a), top panel] undergoes almost 99% fragmentation to 2-allylphenol⁺ and H_2O at the ionization en-

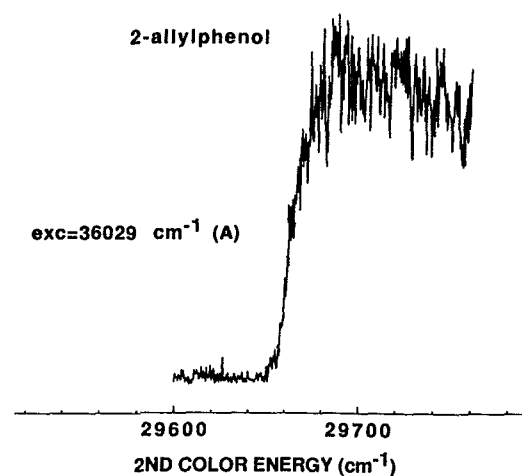


FIG. 2. $I \leftarrow S_1$ threshold photoionization spectrum of 2-allylphenol when the peak A is excited.

TABLE I. Results of the excitation and the threshold ionization spectra for 2-allylphenol.

Excitation frequency (ν_{ex} , cm^{-1})	$I \leftarrow S_1$ onset (ν_{ion} , cm^{-1})	Onset width (cm^{-1})	$\nu_{\text{ex}} + \nu_{\text{ion}}$ (cm^{-1})	Excitation peak assignment
36 029 (peak A)	$29\,662 \pm 4$	28	$65\,691 \pm 4$	Origin I
36 079				Origin I + ν_a (50 cm^{-1})
36 129				Origin I + $2\nu_a$
36 179				Origin I + $3\nu_a$
36 142 (peak B)				Origin I + ν_b (113 cm^{-1})
36 192				Origin I + $\nu_a + \nu_b$
36 242				Origin I + $2\nu_a + \nu_b$
36 251 (peak C)				Origin I + ν_c (222 cm^{-1})
36 301				Origin I + $\nu_a + \nu_c$

ergy employed ($\nu_{\text{ion}} = 30\,650\text{ cm}^{-1}$). The extensive fragmentation is observed until ν_{ion} is lowered to $28\,608\text{ cm}^{-1}$ (lower than the bare molecule threshold).

Unlike the 2-allylphenol/water system for which intense cluster spectra are observed, 2-allylphenol/ammonia clusters yield only very weak one-color MRES, and two-

color MRES are too weak to record. One-color MRES are very broad due to extensive fragmentation. We believe the reason ammonia cluster spectra are so weak is that most of the 2-allylphenol is clustered to impurity water. The water/allylphenol cluster binding energy is roughly twice that of ammonia/allylphenol.

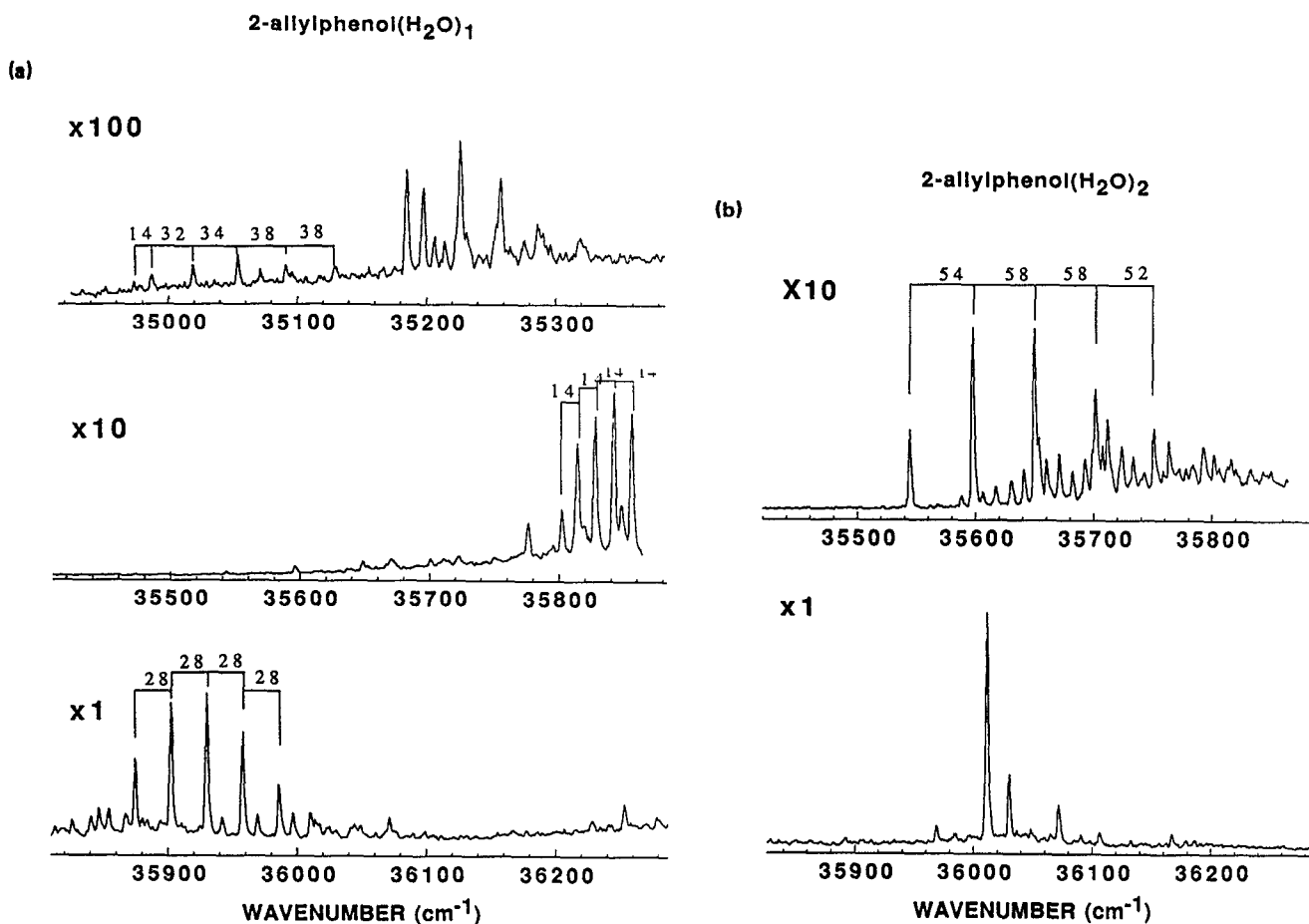


FIG. 3. 2-color MRES of (a) 2-allylphenol(H_2O)₁ and (b) 2-allylphenol(H_2O)₂. Peak intensities are calibrated with dye curves of the excitation laser. Energy of the ionizing laser (ν_{ion}) is $30\,650\text{ cm}^{-1}$.

TABLE II. Summary of threshold ionization energies of 2-allylphenol, 2-propenylphenol, 2-propylphenol clusters.

Sample	Excitation frequency (ν_{ex} , cm^{-1})	$I \leftarrow S_1$ threshold (ν_{ion} , cm^{-1})	Ionization potential (I.P.) ($\nu_{\text{ex}} + \nu_{\text{ion}}$, cm^{-1})	Shift of I.P. from bare molecule I.P. (cm^{-1})
2-allylphenol	36 029	$29\,662 \pm 4$	$65\,691 \pm 4$	0
2-allylphenol(H_2O) ₁	35 873	$27\,268 \pm 50$	$63\,141 \pm 50$	-2550
"	35 853	$26\,968 \pm 50$	$62\,821 \pm 50$	-2870
2-allylphenol(H_2O) ₂	36 006	$26\,968 \pm 50$	$62\,974 \pm 50$	-2717
2-propenylphenol	32 725	$30\,430 \pm 3$	$63\,155 \pm 3$	0
2-propenylphenol(H_2O) ₁	32 284	$27\,380 \pm 50$	$59\,664 \pm 50$	-3491
2-propenylphenol(NH_3) ₁	31 972	$26\,280 \pm 50$	$58\,252 \pm 50$	-4903
2-propenylphenol(NH_3) ₂	31 846	$26\,380 \pm 50$	$58\,226 \pm 50$	-4929
2-propenylphenol(NH_3) ₃	31 861	$25\,748 \pm 50$	$57\,609 \pm 50$	-5546
2-propenylphenol(NH_3) ₄	31 861	$25\,228 \pm 50$	$57\,089 \pm 50$	-6066
2-propylphenol	35 953 ^a	$30\,200 \pm 3$	$66\,153 \pm 3$	0
2-propylphenol(H_2O) ₁	35 607	$26\,380 \pm 50$	$61\,987 \pm 50$	-4166
"	35 871	$26\,210 \pm 50$	$62\,081 \pm 50$	-4072
2-propylphenol(H_2O) ₂	36 092	$27\,255 \pm 50$	$63\,347 \pm 50$	-2806

^a The lowest energy origin.

3. Dispersed emission spectroscopy

Dispersed emission spectra of 2-allylphenol and its clusters with ammonia are presented in Fig. 4. The dispersed emission from 2-allylphenol/water clusters is indistinguishable from that of the "bare molecule" (including, of course, a water contamination, since no mass resolution is employed). The dispersed emission from 2-allylphenol(NH_3)_n is shifted to lower energy: this redshift is usually indicative of an intermolecular excited state proton transfer. The shift in intensity in this instance is small because concentration of 2-allylphenol/ammonia clusters is small as shown above by one- and two-color MRES. The suggestion here is that the transfer is inter- and not intramolecular because the redshifted emission is with respect to both bare molecule and water clusters. The more conclusive evidence with respect to these two possible proton transfer reactions will be provided through comparison between the behavior of the three different chromophores.

4. MOPAC 5 calculations of bare molecule structure

MOPAC 5 calculations for 2-allylphenol are presented in Table III and Fig. 5. Fifteen locally stable conformations are calculated for this molecule. The three most stable conformations are shown in Fig. 5. The single one observed probably corresponds to the lowest energy calculated structure. Interestingly, the syn-conformers ($\tau_3 \sim 180^\circ$) tend in general to be more stable than the anti-conformers ($\tau_3 \sim 0^\circ$). The more stable of the calculated conformers have an interaction between the hydroxyl hydrogen and the allyl group double bond.

5. Potential energy calculations of cluster structure

Calculation of 2-allylphenol/water and ammonia cluster structures is not very reliable because the 2-allylphenol structure is not varied in the clustering process. Nonetheless, through comparison with results of phenol²³ and naphthol¹⁸ clustered with water and ammonia, some general re-

marks can be made. First, most of the clustering takes place at the hydroxyl-allyl site. Second, water molecules tend to bind to one another away from the allylphenol ring and side chain sites. Third, ammonia has a much more distributed geometry about the allylphenol: our cluster potential energy calculations reveal that the ammonia-ammonia interaction ($\sim 500 \text{ cm}^{-1}$) is smaller than the ammonia-allylphenol interaction ($\sim 900 \text{ cm}^{-1}$). Fourth, detailed solute/solvent arrangements are dependent on the solute conformation chosen for clustering. Fifth, the solvent seems to position itself in many cluster configurations in such a fashion as to suggest that the original 2-allylphenol conformer structure would be altered to some extent by the solute/solvent interaction. And sixth, substantial hydrogen bonding takes place between the hydroxyl group and water in which the two possible hydrogen bonding configurations ($\text{OH} \cdots \text{OH}_2$ and $\text{HOH} \cdots \text{OH}$) are of roughly similar ($\sim 1600 \text{ cm}^{-1}$) energy.

B. 2-Propenylphenol

1. MRES and threshold photoionization of the bare molecule

The two-color MRES of 2-propenylphenol near the origin of the $S_1 \leftarrow S_0$ transition is shown in Fig. 6. The feature at $32\,725 \text{ cm}^{-1}$ (A) is the lowest energy and most intense spectral feature and is assigned as the 0_0^0 transition for the anti-isomer (2c). Peaks marked B, C, and E in Fig. 6 are vibrations built on the A origin as can be seen from the threshold photoionization spectra presented in Fig. 7. The sharp onset and large shift in ionization energy for peak D ($33\,491 \text{ cm}^{-1}$) suggest that D is the 0_0^0 transition for the syn-isomer (2b). Table IV presents the threshold photoionization energies for these features: note that the values are the same for features A and D. The assignment of feature D is thus somewhat in question and data for the clusters can be employed to assist in the determination of the nature (i.e., vibronic feature associated with the A 0_0^0 transition, origin I, or 0_0^0 of the syn-isomer 2b).

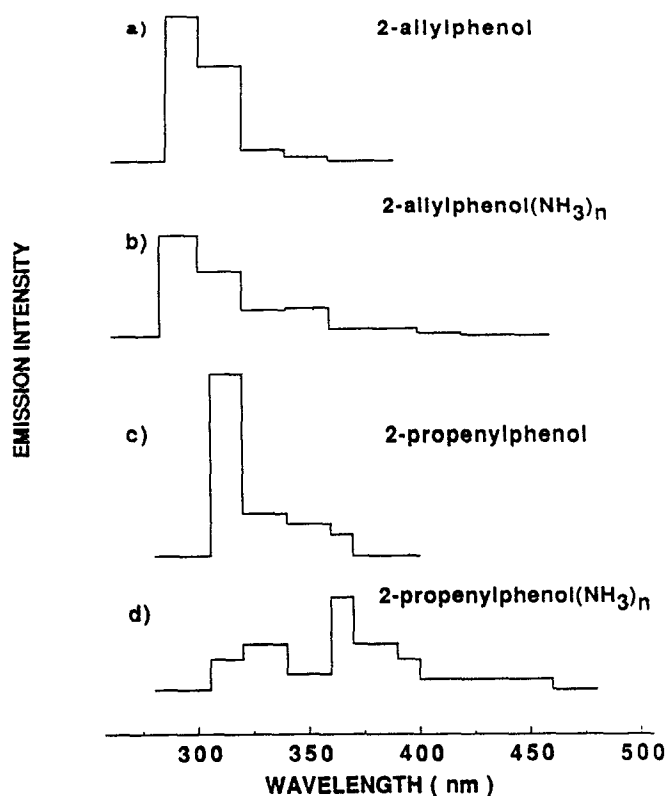


FIG. 4. The dispersed fluorescence emission spectra for (a) 2-allylphenol, (b) 2-allylphenol(NH_3) $_n$, (c) 2-propenylphenol, (d) 2-propenylphenol(NH_3) $_n$. The redshifted emission is obvious for (NH_3) $_n$ clusters. The spectra of (H_2O) $_n$ clusters are similar to the corresponding bare molecule spectrum in terms of wavelength distribution. Filter transmission—(1) UV22–20% @ 200 nm, 40% @ 220 nm, 62% @ 240 nm, 76% @ 260 nm, 86% @ 280 nm, 90% @ > 300 nm. (2) UV28–0% @ < 245 nm, 7% @ 260 nm, 44% @ 280 nm, 77% @ 300 nm, 87% @ 320 nm, 90% @ > 340 nm. (3) UV30–0% < 280 nm, 38% @ 300 nm, 83% @ 320 nm, 90% @ > 350 nm. (4) UV32–0% < 315 nm, 2.5% @ 320 nm, 52% @ 340 nm, 80% @ 360 nm, 84% @ 380 nm, 87% @ > 400 nm. (5) UV36–0% < 340 nm, 47% @ 360 nm, 74% @ 380 nm, 83% @ 400 nm, 86% @ > 420 nm. (6) L38–0% < 355 nm, 47% @ 380 nm, 78% @ 400 nm, 86% @ 420 nm, 90% @ > 460 nm. (7) L40–0% @ < 370 nm, 7% @ 380 nm, 44% @ 400 nm, 71% @ 420 nm, 82% @ 400 nm, 85% @ 460 nm, 87% @ 480 nm, 88% @ > 500 nm. (8) L42–0% < 490 nm, 44% @ 420 nm, 83% @ 440 nm, 87% @ > 460 nm. Filters used for: (a) 2-allylphenol, 2-allylphenol(H_2O) $_n$, 2-allylphenol(NH_3) $_n$, 2-propenylphenol(H_2O) $_n$ —UV22, UV28, UV30, UV32, UV34, UV36, L38. (b) 2-propenylphenol, 2-propenylphenol(H_2O) $_n$, 2-propenylphenol(NH_3) $_n$ —UV30, UV32, UV36, L38, L40, L42.

2. MRES and threshold photoionization of water and ammonia clusters

The two-color MRES of 2-propenylphenol/water and ammonia clusters are presented in Fig. 8. The 1:1 cluster spectra are shifted from the isolated molecule spectra by -442 and -750 cm^{-1} , respectively. These two clusters preserve the isolated molecule vibronic structure and Franck–Condon factors.

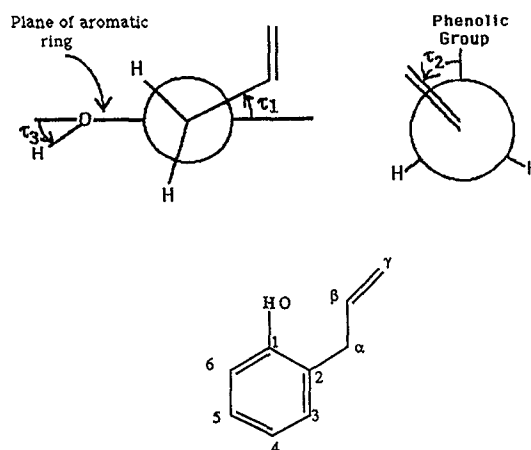
In the 2-propenylphenol(H_2O) $_1$ and (NH_3) $_1$ cluster spectra, peak D (see Fig. 6) is pronounced and unshifted ($\sim 0_0^0 + 768$ cm^{-1}): this suggests that this feature (D in Fig. 6) is vibronic in nature and not the syn-2-propenylphenol as given in 2b.

TABLE III. Conformational energies for 2-allylphenol calculated with MOPAC5/PM3.

τ_3 (degree)	τ_1 (degree)	τ_2 (degree)	ΔH_f (kcal/mol)
178	75	134	-10.4
169	-113	-127	-10.2
176	81	-133	-10.2
174	-38	-141	-9.88
165	-102	-97	-9.74
163	-113	120	-9.72
177	81	0	-9.30
179	65	-69	-9.19
167	-111	17	-8.91
3	95	-130	-8.62
1	84	134	-8.51
3	-13	-149	-8.44
3	26	131	-8.32
1	89	-7	-7.52
0	1	70	-7.37

Definition of τ_1 , τ_2 , τ_3 ; $\tau_1 = \text{angle}(\text{C}_2-\text{C}_3-\text{C}_\alpha-\text{C}_\beta)$, $\tau_2 = \text{angle}(\text{C}_2-\text{C}_\alpha-\text{C}_\beta-\text{C}_\gamma)$, $\tau_3 = \text{angle}(\text{C}_6-\text{C}_1-\text{O}-\text{H})$.

Angles increase in the counterclockwise direction.



2-propenylphenol(H_2O) $_2$ and (NH_3) $_3$ spectra are broad and featureless as are spectra of higher order clusters in these series.

The threshold photoionization values for these clusters are given in Table II. The redshifts of the threshold photoionization values for water clusters appear to reflect only the binding energy differences between the cluster ground and excited states: no large, unexpected changes can be identified that would signify the onset of proton transfer. The behavior of 2-propenylphenol/ammonia clusters is quite similar. For comparison, the ionization energies for indole(H_2O) $_1$, indole(NH_3) $_{1,2}$, for which no proton transfer takes place, are shifted from the isolated indole molecule threshold photoionization energy by -3027 , -4152 , -4529 cm^{-1} , respectively.^{15(e)} One cannot determine if the ~ 600 cm^{-1} redshift of the ionization threshold between 2-propenylphenol(NH_3) $_2$ and (NH_3) $_3$ is due to proton transfer or simply the “usual” binding energy differences for the solvated ions and ground states. The (NH_3) $_3$ to (NH_3) $_4$ shift is comparable and cannot be employed to suggest proton transfer.

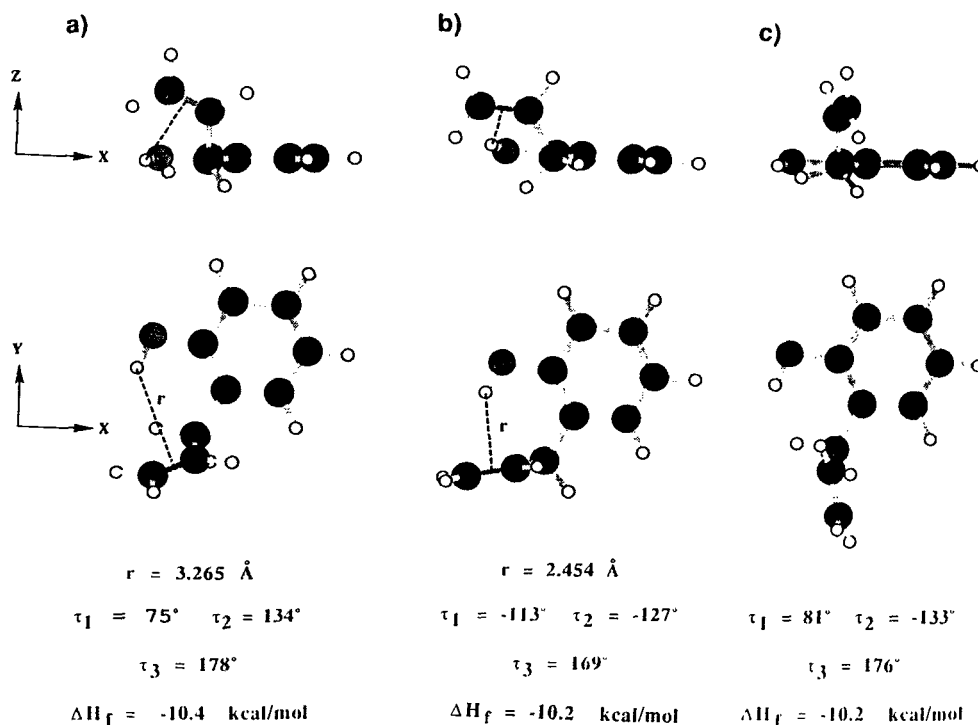


FIG. 5. The three most stable conformations of 2-allylphenol calculated with MOPAC 5/PM3.

3. Dispersed emission

The dispersed emission spectra of 2-propenylphenol and 2-propenylphenol(NH_3)_n are displayed in Figs. 4(c) and 4(d). The water cluster spectra are identical to the bare molecular emission spectrum. The large redshifted emission intensity for the ammonia clusters strongly suggests inter-

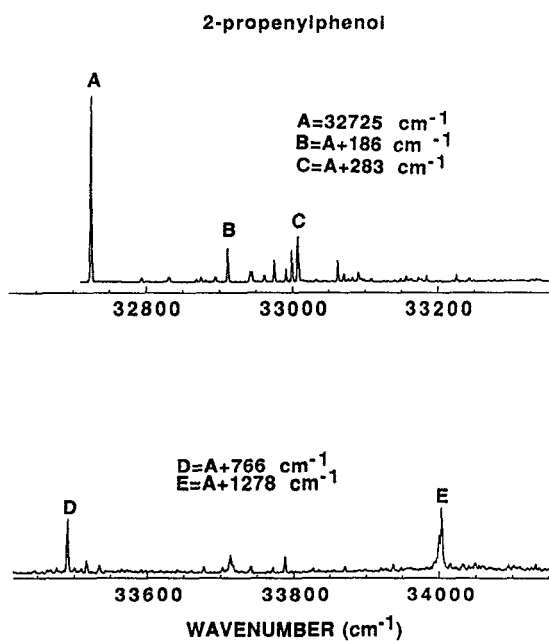


FIG. 6. 2-color MRES of 2-propenylphenol. Peak intensities are calibrated with dye curves of the excitation laser. Energy of ionizing laser (ν_{ion}) is 31 380 cm^{-1} .

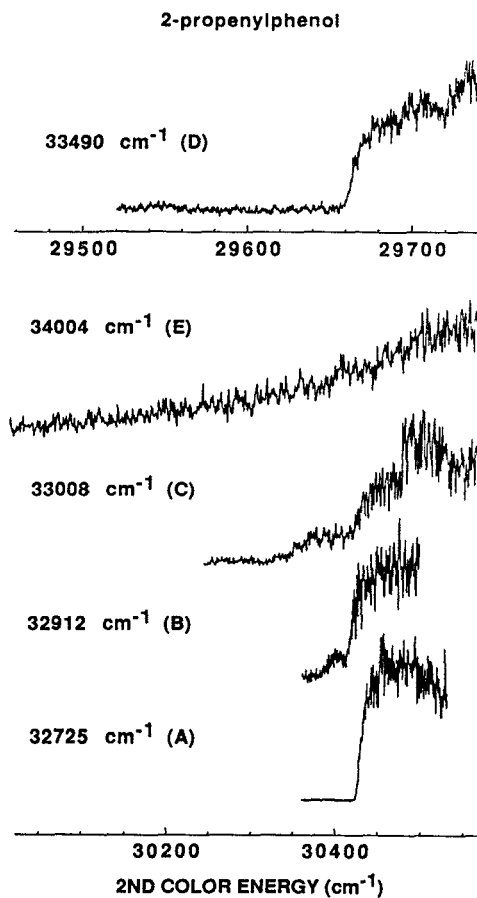


FIG. 7. $I \leftarrow S_1$ threshold photoionization spectra of 2-propenylphenol. Excitation energy is written beside each spectrum.

TABLE IV. Results of the excitation and threshold ionization spectra for 2-propenylphenol.

Excitation frequency (ν_{ex} , cm^{-1})	$I \leftarrow S_1$ onset (ν_{ion} , cm^{-1})	Onset width (cm^{-1})	$\nu_{\text{ex}} + \nu_{\text{ion}}$ (cm^{-1})	Excitation peak assignment
32 725 (peak A)	$30\,430 \pm 3$	14	$63\,155 \pm 3$	Origin I
32 912 (peak B)	$30\,420 \pm 3$	16	$63\,332 \pm 3$	Origin ν_a (187 cm^{-1})
33 008 (peak C)	$30\,432 \pm 10$	120	$63\,440 \pm 10$	Origin I + ν_b (283 cm^{-1})
33 491 (peak D)	$29\,664 \pm 3$	13	$63\,155 \pm 3$	Origin I + ν_c (766 cm^{-1})
34 004 (peak E)	$30\,420 \pm 20$	250	$64\,424 \pm 20$	Origin I + ν_d (1279 cm^{-1})

molecular proton transfer for both 2-allylphenol and 2-propenylphenol(NH_3) $_n$, $n \geq 3$, because (solution phase) intramolecular proton transfer does not take place for the propenylphenol system.⁵⁻⁷ No redshifted emission is found by exciting (NH_3) $_1$ ($31\,972\text{ cm}^{-1}$) and (NH_3) $_2$ ($31\,846\text{ cm}^{-1}$) clusters of 2-propenylphenol.

4. MOPAC 5 calculation of isolated molecule structure

MOPAC 5 PM3 calculation results for 2-propenylphenol are presented in Table V and Fig. 9. For both the syn- and

anti-conformers, the $\tau_3 \sim 180^\circ$ geometry is more stable than the $\tau_3 \sim 0^\circ$ geometry (see Table V for angle definitions). The anti, $\tau_3 \sim 180^\circ$, $\tau_1 \sim 0^\circ$ conformer (see Fig. 9) is the most stable and probably the only one observed in the spectrum. Here too, interaction between the double bond and the hydroxyl group hydrogen is indicated.

5. Potential energy calculations of cluster structure

The results of these cluster calculations are similar to those reported allylphenol/water and ammonia. Hydrogen bonding is stronger for water clusters than ammonia clusters. Both $\text{OH} \cdots \text{OH}_2$ and $\text{HOH} \cdots \text{OH}$ bonding structures are obtained with the latter being $\sim 300\text{ cm}^{-1}$ more tightly bound. The general findings parallel those described above for 2-allylphenol clusters.

TABLE V. Conformational energies for 2-propenylphenol calculated with MOPAC5/PM3.

Isomer	τ_3 (degree)	τ_1 (degree)	ΔH_f (kcal/mol)
Syn	177	110	-14.0
	173	32	-13.8
	0	67	-12.5
	0	34	-12.2
	0	91	-12.1
	8	130	-9.7
Anti	180	1	-16.3
	179	117	-15.2
	0	0	-14.5
	178	143	-14.3
	2	35	-14.1
	1	121	-13.0
	1	176	-12.5

Definition of τ_1 and τ_3 : $\tau_1 = \text{angle}(\text{C}_2-\text{C}_3-\text{C}_\alpha-\text{C}_\beta)$, $\tau_3 = \text{angle}(\text{C}_6-\text{C}_1-\text{O}-\text{H})$, see Table III for numbering. Angles increase in the counterclockwise direction.

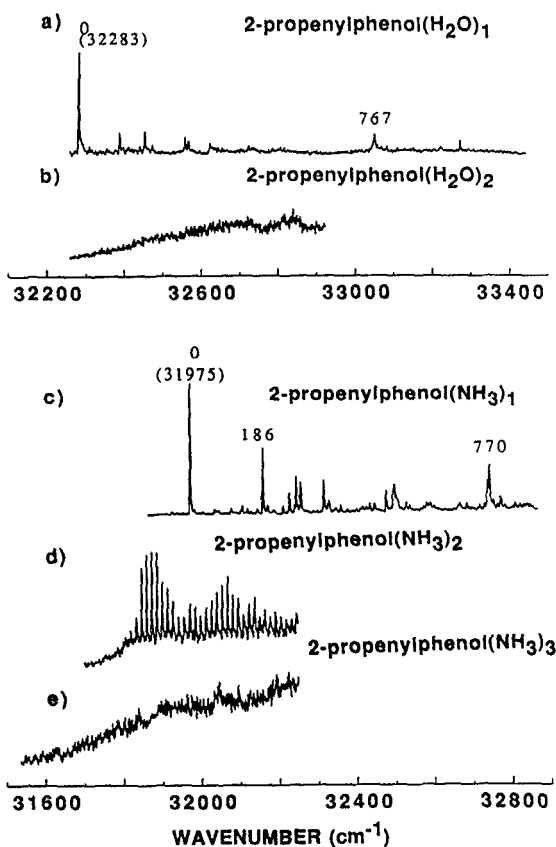
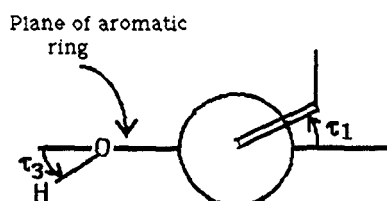


FIG. 8. (a)–(b) 2-color MRES of 2-propenylphenol(H_2O) $_1$ and (H_2O) $_2$. Peak intensities are calibrated with dye curves of the excitation laser. Energy of ionizing laser (ν_{ion}) is $29\,000\text{ cm}^{-1}$. (c)–(e) 2-color MRES of 2-propenylphenol(NH_3) $_{1,2,3}$. Peak intensities are calibrated with dye curves of the excitation laser. Energy of the ionizing laser (ν_{ion}) is $27\,700\text{ cm}^{-1}$. The spectra for higher clusters are featureless and broad.

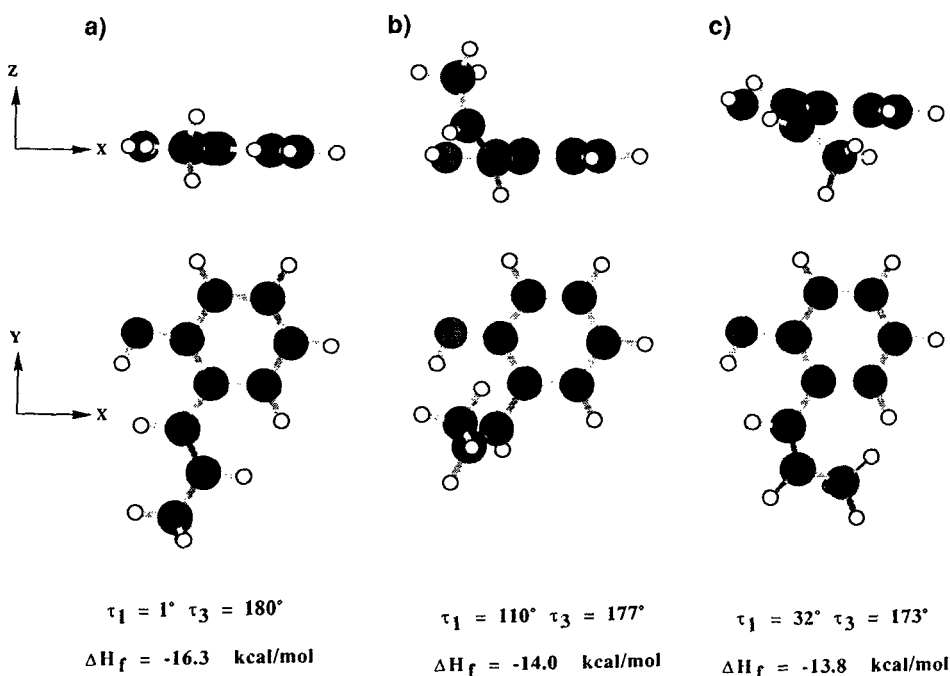


FIG. 9. The most stable geometry of anti-2-propenylphenol (a) and the two most stable conformations of syn-2-propenylphenol (b) and (c).

C. 2-Propylphenol

1. MRES and threshold photoionization of the bare molecule

The two-color MRES of 2-propylphenol about its $S_1 \leftarrow S_0$ origin region is presented in Fig. 10 and its $I \leftarrow S_1$ threshold photo-ionization spectrum is present in Fig. 11 and summarized in Table VI. The features labeled I–V in these spectra and Table VI are most likely 0_0^0 transitions of five conformers of 2-propylphenol: origin transitions of various conformers appear in threshold photoionization as sharp features and vibronic states of conformers appear as broad features. Additionally, as given in Table VI, the fea-

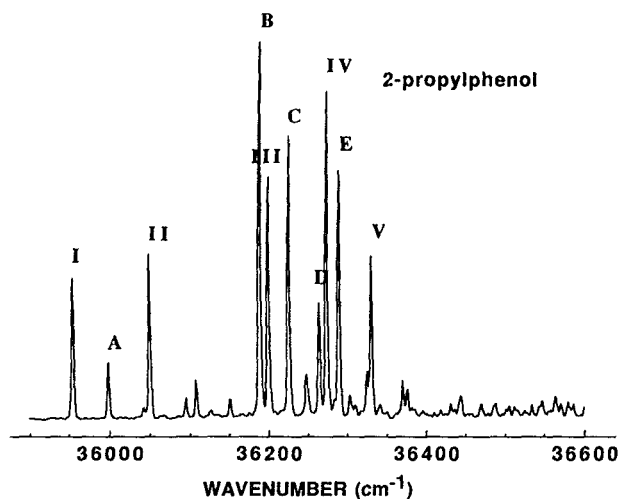


FIG. 10. 2-color MRES of 2-propylphenol. Peak intensities are calibrated with dye curves of the excitation laser. Energy of ionizing laser (ν_{ion}) is $31\,600\text{ cm}^{-1}$.

tures I–V have unique photoionization threshold energies. Firm assignment of the number of origins in this spectrum is not possible, but probably more than five (i.e., I–V and B) can be located.

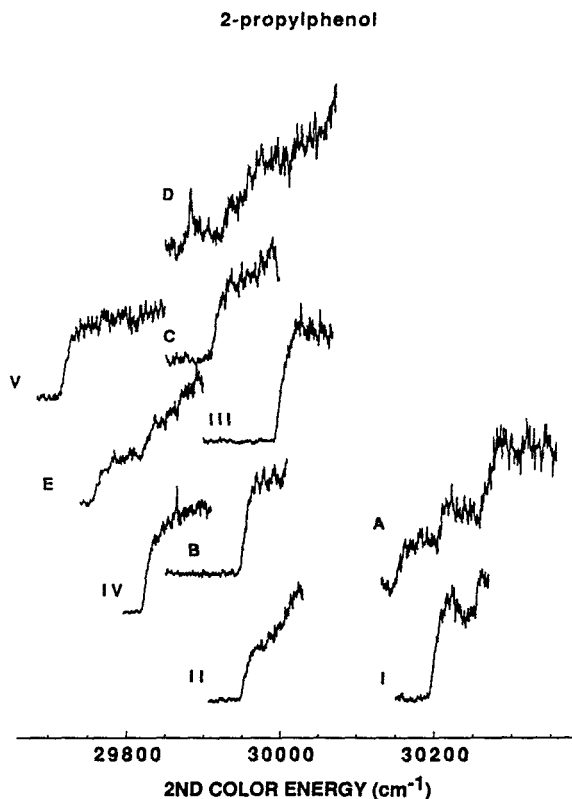


FIG. 11. $I \leftarrow S_1$ threshold photoionization spectra of 2-propylphenol. Excitation energy is written beside each spectrum. (See Fig. 10.)

TABLE VI. Results of the excitation and threshold ionization spectra for 2-propylphenol.

Excitation Frequency (ν_{ex} , cm^{-1})	$I \leftarrow S_1$ onset (ν_{ion} , cm^{-1})	Onset width (cm^{-1})	$\nu_{\text{ex}} + \nu_{\text{ion}}$ (cm^{-1})	Excitation peak assignment
35 953 (peak I)	$30\,200 \pm 3$	17	$66\,153 \pm 2$	Origin I
35 999 (peak A)	$30\,208 \pm 20$	110	$66\,207 \pm 20$	Origin I + 46 cm^{-1}
36 049 (peak II)	$29\,953 \pm 3$	17	$66\,002 \pm 3$	Origin II
36 189 (peak B)	$29\,954 \pm 2$	17	$66\,143 \pm 3$? (A new origin or origin II + 140 cm^{-1})
36 199 (peak III)	$30\,001 \pm 2$	18	$66\,200 \pm 2$	Origin III
36 226 (peak C)	$29\,916 \pm 3$	14	$66\,142 \pm 3$? (A new origin or peak B + 47 cm^{-1})
36 263 (peak D)	$29\,950 \pm 20$	80	$66\,213 \pm 20$	A vibration
36 273 (peak IV)	$29\,825 \pm 2$	13	$66\,098 \pm 2$	Origin IV
36 288 (peak E)	$29\,827 \pm 20$	110	$66\,115 \pm 20$	Origin IV + 15 cm^{-1}
36 239 (peak V)	$29\,722 \pm 2$	15	$66\,051 \pm 2$	Origin V

2. MRES and threshold photoionization of water and ammonia clusters

The two-color MRES spectra of 2-propylphenol(H_2O)_{1,2} clusters are presented in Figs. 12(a) and 12(b). Only one-color MRES are obtained for (NH_3)_n clusters due to their low concentration in the expansion. Due to the large number of possible 2-propylphenol molecule conformers, many cluster conformations are possible for each specific cluster mass. 2-propylphenol(H_2O)_n, $n = 1, 2$, threshold photoionization data are presented in Table II. Ammonia cluster spectra are too weak to generate meaningful results for threshold photoionization.

3. Dispersed emission

Almost all emission observed from 2-propylphenol samples, whether expanded with ammonia or not, comes from 2-propylphenol(H_2O)_n. Vacuum drying of the sample did not seem to change this significantly. Some changes in the red emission with high concentrations of ammonia may be present but they are difficult to quantify. The impurity water/2-propylphenol ratio is probably 1:1 and water binds to the phenol to exclude other solvents (binding energy for $\text{H}_2\text{O} \sim 1600 \text{ cm}^{-1}$ and for $\text{NH}_3 \sim 800 \text{ cm}^{-1}$ based on our cluster potential energy calculations).

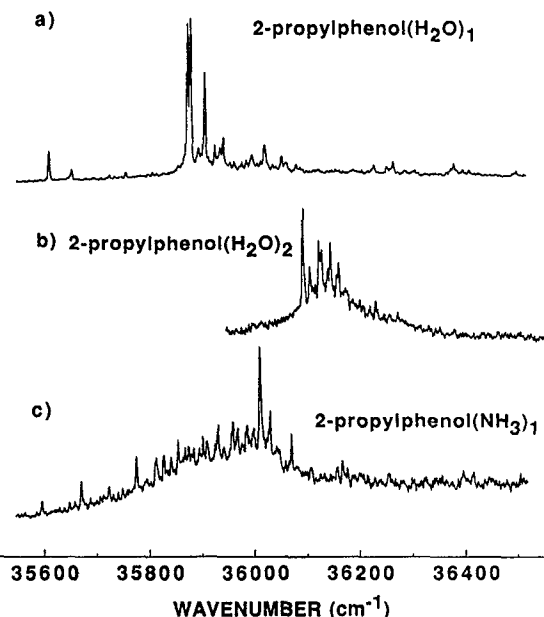


FIG. 12. (a)–(b) 2-color MRES of 2-propylphenol(H_2O)₁ and (H_2O)₂. Peak intensities are calibrated with dye curves of the excitation laser. Energy of ionizing laser (ν_{ion}) is $29\,960 \text{ cm}^{-1}$. (c) 1-color MRES of 2-propylphenol(NH_3)₁. Peak intensities are calibrated with dye curves of the excitation laser. The spectra for higher clusters are featureless and broad.

4. MOPAC 5 calculations of molecular structure

Seven different low energy structures are found for the 2-propylphenol system. The calculation still prefers syn-(OH) conformations over anti-(OH) conformations, but the energy differences are now quite small. The potential surface for this molecule is clearly very complex and the molecule is probably quite flexible with regard to hydroxyl and propyl group orientations and displacements.

No cluster detailed calculations are presented for this system. The general conclusions for cluster structure follow from the remarks made for the other two molecules in this study. Binding energies for water are $\sim 1500 \text{ cm}^{-1}$ and for ammonia $\sim 800 \text{ cm}^{-1}$. Cluster formation can dramatically change and/or interconnect any of the local minima presented in Table VII because the potential energy surface around the local minima is so shallow.

IV. DISCUSSION

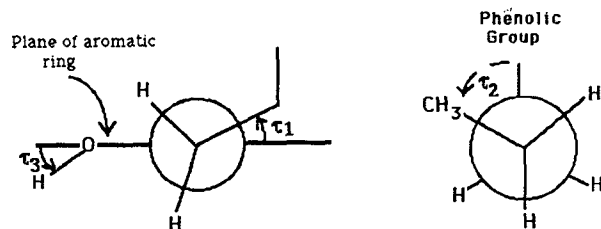
A. 2-Allylphenol

Experimental and calculational evidence presented in the last section is consistent with a reasonably strong internal hydrogen bond between the hydroxyl hydrogen and the terminal allyl group double bond (see Fig. 5) yielding a low energy single 2-allylphenol molecular conformation. Note that 2-methyl-allylbenzene displays two conformers.^{24,25}

The 50 cm^{-1} vibronic progression following the origin transition is not related to OH group motion, but to a change in orientation of the allyl group upon electronic ($S_1 \leftarrow S_0$) excitation (see Fig. 1). Most likely this change is associated with the large change in pK_a of the hydroxyl proton upon electronic excitation and the concomitant increase in hydro-

TABLE VII. Conformational energies for 2-propylphenol calculated with MOPAC5/PM3.

τ_3 (degree)	τ_1 (degree)	τ_2 (degree)	ΔH_f (kcal/mol)
175	85	181	-41.0
181	76	72	-40.4
175	88	-75	-40.1
192	100	111	-39.8
2	83	181	-39.1
2	95	-75	-38.5
0	75	75	-38.2



gen bonding strength between the groups. Such a change is not observed in other allylbenzene species.¹⁰

The ionization potential for 2-allylphenol ($65\,690\text{ cm}^{-1}$) is not particularly low compared to those for 2-propenyl- and 2-propylphenol ($63\,155$ and $66\,100 \pm 100\text{ cm}^{-1}$, respectively). Thus intramolecular proton transfer in bare molecule 2-allylphenol is not indicated by these data: a redshifted ionization threshold would be expected for internal proton transfer.

Dispersion emission for bare 2-allylphenol is also not particularly redshifted compared to that of the other species. We conclude that intramolecular proton transfer is absent in the bare 2-allylphenol molecule.

Neither water clusters nor small ($n < 3$) ammonia clusters show dramatic redshifts for ionization thresholds or $S_1 \rightarrow S_0$ emission: proton transfer (internal or external) does not occur for these systems either.

Redshifted emission is found for 2-allylphenol(NH_3) $_n$, $n \geq 3$. Since the redshift is similar to that reported for naphthol/ammonia systems^{1(d),1(e)} and similar to that for 2-propenylphenol/ammonia clusters (no internal proton transfer identified for 2-propenylphenol even in solution), we conclude that intermolecular excited state proton transfer has occurred in 2-allylphenol(NH_3) $_n$, $n \geq 3$.

As pointed out above and in a previous publication,¹⁸ ammonia (for $n > 3$) is much better at solvation of *both* the anion and the proton than is water. The interaction between the ammonia molecules and the chromophore is distributed over the entire cluster because ammonia is a (relatively) poor hydrogen bond donor and the ammonia/ammonia interaction is only $\sim 500\text{ cm}^{-1}$. Water, on the other hand, hydrogen bonds to the hydroxyl proton and itself ($\sim 1500\text{ cm}^{-1}$) and mostly avoids the remainder of the chromophore in its low energy cluster geometries.

B. 2-Propenylphenol

Calculated geometries for this molecule suggest that the propenyl double bond and the hydroxyl hydrogen interact only weakly. This is consistent with the absence of internal

proton transfer in solution and absence of a vibrational progression in either propenyl or hydroxyl motion following the 0_0^0 transition. All of this is consistent with threshold photoionization data: no special redshifts can be identified.

Cluster emission results are consistent with excited state proton transfer for $n \geq 3$ but not for $n < 3$ in 2-propenylphenol/ammonia clusters. Again, only the dispersed emission evidences any proton transfer behavior. Comparisons with 2-allylphenol require the transfer in both instances to be intermolecular. Cluster structure calculations generate a reasonable explanation for the difference in behavior between water and ammonia clusters. Intermolecular proton transfer in the excited state is favored if both ions can be well solvated, as must happen in any event in solution due to solvent crowding and packing.

Threshold photoionization energies in this cluster system do not appear to change dramatically, over and above the general clustering trends, for $n \geq 3$ ammonia clusters; however, emission data for these clusters indicate intermolecular proton transfer has occurred. In general, one must employ a number of detection techniques to identify chemical reactions in clusters.

C. 2-Propylphenol

Cold, isolated 2-propylphenol can have many conformations: calculations of molecular structure also yield a number of nearly equivalent (e.g., 500 cm^{-1}) local energy minima on the ground state potential surface. Interactions between the propyl moiety and the hydroxyl group seem to be favored even though no side chain π system is present.

Experimental difficulties with water contamination make ammonia clusters of 2-propylphenol difficult to detect but weak emission data suggest that proton transfer can occur for the larger ($n \geq 3$) ammonia clusters of 2-propylphenol.

D. Proton transfer in clusters and solvation

Proton transfer occurs in small solute/solvent clusters if the solvent and solvation geometry are appropriate. The results of these studies seem to emphasize solvent proton affinity, solvent-solvent, and solvent-solute interaction energy, detailed solvent geometry around the solute, and the number of solvent molecules in the cluster. Most likely, some combination of these properties finally determines whether or not proton transfer occurs in a given cluster.

VI. CONCLUSIONS

Based on two-color mass resolved excitation, dispersed emission, threshold photoionization spectroscopies, semiempirical MNDO, and cluster potential energy calculations, for 2-allyl, 2-propenyl-, and 2-propylphenol and their clusters with water and ammonia, we can conclude the following:

- (1) no *intramolecular* proton transfer occurs in any (isolated molecule or cluster) of these systems;
- (2) no *intermolecular* proton transfer occurs for clusters with $(\text{H}_2\text{O})_n$ or $(\text{NH}_3)_{1,2}$;
- (3) *intermolecular* excited state proton transfer occurs

for larger clusters ($n \geq 3$) of ammonia with 2-allyl- and 2-propenylphenol;

(4) intermolecular excited state proton transfer may occur for 2-propylphenol(NH_3) $_n$, $n \geq 3$, but impurity water clustering makes this determination less certain than for the other chromophore species;

(5) in all three of these species the isolated molecules appear to have a significant interaction between the hydrocarbon side chain and the hydroxyl group hydrogen;

(6) if this latter "hydrogen bonding" interaction is strong (e.g., 2-allyl- and 2-propenylphenol), only one molecular conformer is present in the expansion, but if it is weak (e.g., 2-propylphenol), the molecular potential energy surface has many accessible nearly equivalent energy minima;

(7) for excited state proton transfer to occur at a given cluster size (e.g., $n > 3$) a combination of adequate ion solvation (both proton and anion) and good solvent proton affinity is required; and

(8) cluster chemical reactions may be detected by dispersed emission, threshold photoionization, and/or two-color mass resolved excitation spectroscopies depending on the system under investigation.¹⁸

ACKNOWLEDGMENTS

This work was supported in part by grants from the Office of Naval Research and the National Science Foundation.

¹ (a) J. J. Breen, L. W. Peng, D. M. Willberg, A. Heikal, P. Cong, and A. H. Zewail, *J. Chem. Phys.* **92**, 805 (1990); D. H. Semmes, J. S. Baskin, and A. H. Zewail, *ibid.* **92**, 3359 (1990); A. H. Zewail, *Science* **242**, 1645 (1988). References to earlier studies can be found in these three references; (b) J. A. Syage, *ibid.* **92**, 1804 (1990), and J. Steadman, J. A. Syage, *ibid.* **92**, 4630 (1990); (c) C. Wittig, S. Sharpe, and R. H. Beaudet, *Acc. Chem. Res.* **21**, 341 (1988); (d) O. Cheshnovski and S. Leutwyler, *J. Chem. Phys.* **88**, 4127 (1988); (e) T. Dorz, R. Knochenmuss, and S. Leutwyler, *ibid.* **93**, 4520 (1990).

² T. Förster, *Chem. Phys. Lett.* **17**, 309 (1972).

³ J. F. Ireland and P. A. H. Wyatt, *Adv. Phys. Ors. Chem.* **12**, 131 (1976).

⁴ W. Bartok, P. J. Lucchesi, and N. S. Snider, *J. Am. Chem. Soc.* **84**, 1842 (1962).

⁵ G. Frater and H. Schmid, *Hel. Chim. Act.* **50**, 255 (1967).

⁶ S. Houry, S. Geresh, and A. Shani, *Isr. J. Chem.* **11**, 805 (1973).

⁷ S. Geresh, O. Levy, Y. Markovits, and A. Shani, *Tetrahedron* **31**, 2803 (1975).

⁸ N. R. Davies and A. D. DiMichiel, *Aust. J. Chem.* **26**, 1529, (1973).

⁹ (a) H. Abe, N. Mikami, and M. Ito, *J. Phys. Chem.* **86**, 1768 (1982); (b) H. Abe, N. Mikami, M. Ito, and Y. Udagawa, *ibid.* **86**, 2567 (1982), and *Chem. Phys. Lett.* **93**, 217 (1982); (c) A. Oikawa, H. Abe, N. Mikami, and M. Ito, *J. Phys. Chem.* **87**, 5083 (1983); **88**, 5180 (1984); (d) H. Mizuno, K. Okuyama, T. Ebata, and M. Ito, *ibid.* **91**, 5589 (1987).

¹⁰ P. J. Breen, E. R. Bernstein, J. I. Seeman, and H. V. Secor, *J. Phys. Chem.* **93**, 6731 (1989).

¹¹ H. S. Im, E. R. Bernstein, and J. I. Seeman, *J. Chem. Phys.* (to be published).

¹² J. I. Seeman, H. V. Secor, P. J. Breen, V. H. Grassian, and E. R. Bernstein, *J. Am. Chem. Soc.* **111**, 3140 (1989).

¹³ (a) R. Nowak, J. A. Menapace, and E. R. Bernstein, *J. Chem. Phys.* **89**, 1309 (1988); (b) J. A. Warren, E. R. Bernstein, and J. I. Seeman, *ibid.* **88**, 871 (1988); (c) V. H. Grassian, E. R. Bernstein, H. V. Secor, and J. I. Seeman, *J. Phys. Chem.* **93**, 3470 (1989); (d) H. S. Im, V. H. Grassian, and E. R. Bernstein, *ibid.* **94**, 222 (1990); (e) H. S. Im, E. R. Bernstein, J. I. Seeman, and H. V. Secor, *J. Am. Chem. Soc.* (to be published); (f) J. I. Seeman, H. V. Secor, H. S. Im, and E. R. Bernstein, *ibid.* **112**, 7073 (1990).

¹⁴ R. J. Lipert and S. D. Colson, *J. Phys. Chem.* **93**, 3894 (1989).

¹⁵ (a) M. A. Duncan, T. G. Dietz, and R. E. Smalley, *J. Chem. Phys.* **75**, 2118 (1981); (b) J. Hager, M. A. Smith, and S. C. Wallace, *ibid.* **83**, 4820 (1985); **84**, 6771 (1986); (c) J. Hager, M. A. Smith, and S. C. Wallace, *ibid.* **89**, 3833 (1985); (d) J. Hager, M. Ivanco, M. A. Smith, and S. C. Wallace, *Chem. Phys. Lett.* **113**, 503 (1985); (e) J. Hager, M. Ivanco, M. A. Smith, and S. C. Wallace, *Chem. Phys.* **105**, 397 (1986); (f) J. Hager, G. W. Leach, D. R. Demmer, and S. C. Wallace, *J. Phys. Chem.* **91**, 3750 (1987).

¹⁶ D. Solgadi, C. Jouviet, and A. Tramer, *J. Phys. Chem.* **92**, 3313 (1988).

¹⁷ C. Jouviet, C. Lardeux-Dedonder, M. Richard-Viard, D. Solgadi, and A. Tramer, *J. Phys. Chem.* **94**, 5041 (1990).

¹⁸ S. K. Kim, S. Li, and E. R. Bernstein, *J. Chem. Phys.* **95**, 3119 (1991).

¹⁹ (a) J. Wanna and E. R. Bernstein, *J. Chem. Phys.* **84**, 927 (1986); (b) J. Wanna, J. A. Menapace, and E. R. Bernstein, *ibid.* **85**, 777 (1986); (c) J. Wanna, J. A. Menapace, and E. R. Bernstein, *ibid.* **85**, 1795 (1986); (d) J. Wanna and E. R. Bernstein, *ibid.* **85**, 3243 (1986).

²⁰ E. R. Bernstein, K. Law, and M. Schauer, *J. Chem. Phys.* **80**, 207 (1984).

²¹ J. J. P. Stewart, *J. Comput. Chem.* **10**, 209 (1989).

²² (a) P. J. Breen, J. A. Warren, E. R. Bernstein, and J. I. Seeman, *J. Chem. Phys.* **87**, 1972 (1987); (b) J. A. Menapace and E. R. Bernstein, *J. Phys. Chem.* **91**, 2843 (1987); (c) M. R. Nimlos, D. F. Kelley, and E. R. Bernstein, *ibid.* **93**, 643 (1989).

²³ S. Li, S. K. Kim, E. R. Bernstein (unpublished results).

²⁴ T. Schaefer, R. Sebastian, and T. A. Wildman, *Can. J. Chem.* **57**, 3005, (1979).

²⁵ M. Oki and H. Iwamura, *Bull. Chem. Soc. Jpn.* **33**, 717 (1960).